INVENTORY OF SUPPLEMENTAL INFORMATION

Supplemental Table 1. Patient characteristics for the cohort of 122 individuals from Figure S1 receiving an allograft from HLA-matched sibling donors. (A) Distribution of the *ATG16L1* WT and T300A alleles in transplant donor and recipients. **(B)** Distribution of the causes of non-relapse mortality (NRM) in Figure S1. Major GVHD is defined as grade III or IV

according to the Glucksberg criteria (Glucksberg et al., 1974). Although a cohort of an additional 69 patients receiving an allograft from unrelated donors was available during the period of this study, the effect of *ATG16L1*^{T300A} on NRM could not be analyzed due to a high incidence of tumor-relapse in this group.

Supplemental Table 2. Microarray analyses of DCs from untreated and allo-HSCT recipient WT and Atg16L1^{HM} mice. First tab shows complete gene list where fold change refers to Atg16L1^{HM} over WT at steady state levels. Second tab shows GSEA analysis of leading edge genes from WT high and Atg16L1^{HM} high gene sets. Third tab shows complete gene list where fold change refers to Atg16L1^{HM} over WT after allo-HSCT. Fourth tab shows GSEA analysis of leading edge genes from Atg16L1^{HM} high and WT allo-HSCT recipients high gene sets.

Supplemental Figure 1, related to Figure 1. Atg16L1 mutation increases morbidity and mortality after allo-HSCT with altered levels of pro-inflammatory cytokines. (A−B) Lethally-irradiated WT and Atg16L1^{HM} recipients were transplanted with TCD-BM cells with and without a lower dose of splenic T cells (1x10^6) from donor B10.BR mice and monitored for (A) survival and (B) weight loss. *n* = 10 recipient mice/group. **(C)** WT mice in the B10.BR→B6 allo-HSCT model typically display more lethality than we observed in Figure 1A. The allo-HSCT from Figure 1A was repeated in a second animal facility (Memorial Sloan Kettering Cancer Center) to examine if the degree of lethality was facility-dependent. In contrast to the original experiment (performed in the ultra-clean animal room at New York University School of Medicine), WT recipients displayed substantial lethality. However, Atg16L1^{HM} recipients remained significantly more susceptible. *n* = 10 recipient mice/group. **(D-E)** Cytokine and chemokine levels were measured by multiplex ELISA (Millipore) using serum from mice receiving the allo-HSCT described in Figure 1A-C on day 7 after the transplantation. Results were acquired with a Luminex 200

instrument and analyzed with xPONENT software. Cytokines displaying increases in Atg16L1^{HM} allo-HSCT recipients are shown in C and those displaying decrease are shown in D. Untreated WT mice 6-weeks of age were used as additional controls to show baseline cytokine levels. No significant differences were seen in IL-1α, IL-1β, IL-2, IL-4, IL-15, IL-10, IL-13, IL-6, IL-17, IP-10, and RANTES when comparing B6 mice and Atg16L1^{HM} receiving TCD-BM + T cells. *n* = 5-9 mice/group. **(F)** Survival of WT and Atg16L1^{HM} treated with 500 μg of anti-TNFα or Isotype control (BioXcell) by i.p. injection on days -1 and 0, and every other day thereafter. Mice were transplanted with TCD-BM cells with 2x10^6 splenic T cells from donor B10.BR mice on day 0 as in Figure 1A-C. *n* = 10 mice/group. **(G)** Serum FITC-dextran concentration following oral gavage was measured in WT and Atg16L1^{HM} mice on day 7 after lethal irradiation. (**H-I**) 122 donor-recipient pairs receiving allo-HSCT from HLA-identical sibling either at the University of Regensburg (*n* = 47, from May, 2000 until May, 2012) or at the University of Newcastle (*n* = 75, from January, 1993 until December, 2007) were included. Collection of samples for genotyping was approved by local ethical committees at both sites. DNA was typed for presence or absence of the *ATG16L1^{T300A}* allele as described previously (Latiano et al., 2008). Results of genotyping were compared with major patient characteristics and outcome variables such as GVHD, non-relapse mortality (NRM), and overall survival using a SPSS based database and PASW statistic software for analysis. NRM and overall survival were calculated by Kaplan-Meier analysis, and Cox regression was used to compare risk factors in multivariate analysis. Patients receiving allo-HSCT from HLA-identical siblings were analyzed. DNA from patients and donors was isolated and typed for presence (heterozygous or homozygous) or absence of the *ATG16L1^{T300A}* allele. The effect of the risk allele in donors and recipients were analyzed separately. (**H**) Rate of non-relapse mortality (NRM) in allo-HSCT recipients when the *ATG16L1^{T300A}* allele is present versus absent in the donor. (**I**) Rate of NRM in allo-HSCT recipients when the *ATG16L1^{T300A}* allele is present versus absent in the recipient. *n* = 6

mice/group. Mean ± S.E.M. are shown in (B), (D)-(E), and (G). *P < 0.05, **P < 0.01, ***P < 0.001.

Supplemental Figure 2, related to Figure 2. Histopathology of allo-HSCT recipients in the intestine and skin. **(A-F)** H&E-stained tissue sections from WT and Atg16L1^{HM} allo-HSCT recipients (TCD-BM and 2x10^6 T cells as in Figure 1 A-C) on day 7 were processed and examined for histopathology as previously described (Cadwell et al., 2010; Penack et al., 2009). Representative images of (A) small intestine and (B) skin, and blind quantification of GVHD histopathology using previous described parameters (Petrovic et al., 2004) shown for (C) small intestine, (D) colon, (E) liver, and (F) skin. Magnification: x10 for small intestines, x40 for skin. (**G-J**) Quantification of histopathology as described above on day 14-post allo-HSCT with a lower dose of T cells (1x10^6 T cells) to allow survival of mice. *n* = 6-8 mice/group. Mean ± S.E.M. are shown in (C-J).

Supplemental Figure 3, related to Figure 3. DCs from Atg16L1^{HM} mice display an altered transcriptional profile. **(A-D)** Additional microarray analyses corresponding to the experiments described in Figure 3B and 3C. Heat-map presentation of gene-expression profiles after Significance Analysis of Microarray (SAM) (Z-score > 2) for (A) allo-HSCT recipients and (C) untreated mice. Complete list of genes can be found in Supplementary Table 2. Bar graphs in (B) and (D) represent p-values for biological processes (GO terms) displaying the most significant enrichment in Atg16L1^{HM} allo-HSCT recipient and untreated Atg16L1^{HM} mice compared to their respective WT controls. Enrichment in GO terms was determined by DAVID (Database for Annotation, Visualization and Integrated Discovery) using Z > 2 cutoff.

Supplemental Figure 4, related to Figure 4. Atg16L1 functions within DCs to prevent hyperactivity. **(A-D)** Flow cytometric analyses of small intestinal lamina propria cells from

untreated or lethally (1100 cGy) irradiated WT and Atg16L1^{HM} mice. CD3^{-}B220^{-}NK1.1^{-}class-II^{+} CD11c^{+} cells were gated on either (A, B) CD11b^{-}CD103^{+} or (C, D) CD11b^{+}CD103^{+}. MFI quantification shown for CD80 (A and C) and CD86 expression (B and D). No significant differences were noted when gating on percent cells that are CD80^{+} or CD86^{+}, and there were no difference in cell numbers. **(E-F)** Similar flow cytometric analyses of mesenteric lymph nodes (MLNs) from untreated WT or Atg16L1^{HM} mice. **(G)** Western blot comparing Atg16L1 levels (Sigma: A7356) in sorted splenic DCs from control (Atg16L1$^{flox/flox}$) and Atg16L1$^{\Delta CD11c}$ mice. **(H)** Clinical GVHD score of allo-HSCT recipient Atg16L1$^{\Delta CD11c}$ mice from Figure 4I. **(I)** Quantification of indicated splenic DC subsets by flow cytometry from Atg16L1$^{\Delta CD11c}$ and control mice 24 hours after lethal irradiation. *n* = 3 mice/group. **(J)** Flow cytometry analysis of CD80 expression on CD11c^{+} splenic cells isolated from Atg16L1$^{\Delta CD11c}$ and control mice that were cultured for 24 hours. n = 3-4 mice/group. Mean ± S.E.M. are shown in (A)-(F) and (H)-(J). **P* < 0.05.

Supplemental Figure 5, related to Figure 5. Increased co-stimulatory molecule expression on Atg16L1-deficient DCs is not transferrable. (A) ^{3}H-thymidine incorporation of allogeneic B10.BR T cells co-cultured at a 1:1 ratio for 72 hours with DCs purified from the spleen of WT and Atg16L1^{HM} mice, with or without neutralizing antibodies against IL-1β (5 μg/mL), anti-IL-1R1 (0.5 μg/mL), or anti-IL-12 (1 μg/mL) (R&D systems). **(B)** Flow cytometric analysis of CD80 expression on WT DCs cultured for 24 hours in supernatant collected from previously cultured Atg16L1^{HM} DCs. **(C, D)** Flow cytometric analysis of CD11c^{+} DCs cultured with GM-CSF for 24 hours and stained for the ROS-detecting cell permeable dyes (C) dihydroethidium (DHE) and (D) 2',7'-dichlorodihydrofluorescein diacetate (DCFDA). *n* = 3 mice/condition. Bar graphs represent mean ± S.E.M and *n* = 3-6 mice/condition. *****P* < 0.0001.

Supplemental Figure 6, related to Figure 6. Atg16L1 deficiency results in lysosomal abnormalities and decreased A20 expression. (A, B) Quantification of lysosomes,

dysmorphic lysosomes, and multivesicular bodies detected per cell by TEM in splenic DCs harvested from (A) untreated mice or (B) mice 24 hrs after lethal irradiation. **(C, D)** Quantification of the percentage of vesicles detected per cell by TEM in splenic DCs harvested from (A) untreated mice or (B) mice 24 hrs after lethal irradiation. **(E)** qRT-PCR analysis of Laptm5 expression in splenic DCs from WT and Atg16L1^{HM} mice cultured in GM-CSF containing media for 24 hrs. 5-7 mice/genotype. (**F**) Representative Western blot analyses of A20, phospho-IkB, phospho-JNK, and actin in whole cell lysates from DCs cultured as in (E). **(G)** Quantification of Western blot from (F). 6 mice/genotype. Bar graphs represent mean ± S.E.M, *P < 0.05, **P < 0.01, ****P < 0.0001. **(H)** Model figure: By inhibiting NF-κB and MAPK signaling, A20 prevents unregulated co-stimulatory molecule expression in DCs exposed to environmental stressors. In Atg16L1-deficient cells, decreased autophagy leads to accumulation of aberrant lysosomal structures and an accompanying lysosomal transcriptional response including enhanced expression of Laptm5. Laptm5 accumulation then mediates the degradation of A20 causing increased expression of the co-stimulatory molecules CD80, CD86, and CD40 that mediate enhanced T cell alloreactivity and subsequent GVHD.

SUPPLEMENTAL METHODS

Assaying for intestinal permeability. Mice were maintained without food and water for 4 hrs and then orally gavaged with 40 mg/ml FITC-dextran (#FD4-1G, Sigma) in 400 ml PBS (16 mg). 4 hrs later, plasma was collected from peripheral blood, then mixed 1:1 with PBS and analyzed on a plate reader at an excitation wavelength of 485 nm and an emission wavelength of 535 nm. Translocated bacteria were quantified by plating serially diluted whole blood or spleen homogenized in sterile thioglycollate medium on blood agar plates incubated at 37 °C for 24 hrs.

Cell culture. MLR was performed as previously described (Penack et al., 2009) using either splenic DCs or BM-differentiated DCs (BMDCs). Splenic DCs were enriched by CD11c^{+}

selection (Miltenyi MACS) and then incubated with allogeneic T cells with 1:1 ratio for 48-96 hrs. Thymidine (1mCi [0.037 MBq] [^{3}H]thymidine/well) was added during the last 18 hrs of incubation and uptake was measured (TopCount, Packard). BMDCs were isolated from femurs and tibias of mice and cultured in media supplemented with 20 ng/mL GM-CSF (Peprotech) for 4 days. 1μg/mL LPS (Sigma-UltraPure) was added 24 hrs before starting co-culture with allogeneic T cells. Relative proliferation was determined by normalizing data to the mean WT value, and each condition was performed in triplicate. For other culture experiments, DCs were plated on 96 well TC-treated plates for indicated times in complete DMEM (10% FCS, 1% penicillin/streptomycin, 1% Glutamine and 10mM HEPES) with 20ng/mL GM-CSF added. For Western blot analyses, total cellular lysates were prepared using RIPA buffer (1% Triton-X 100, 1% sodium deoxycholate, 0.1%SDS, 0.15 M NaCl, 0.01 M sodium phosphate, pH 7.2). Membranes were incubated with the following primary antibodies: LC3, (Sigma, clone 2H30L32), p62 (Sigma clone P0067), A20, (Cell Signaling, clone D13H3), phosphor-IκB (Cell Signaling 14D4), phosphor-JNK (Cell Signaling, E1811), and Actin (AbCam). Quantification of bands was performed using ImageJ software. Chemical inducers of autophagy were from Sigma.

Microscopy. For analysis of LC3 dot formation by florescence microscopy, CD11c$^+$ isolated splenic cells were stimulated on glass bottom microwell dishes (MatTek) with or without GM-CSF +/- 20mM of NH_4CL for 5 hrs. Cells were fixed with 4% paraformaldehyde, permeabilized with 0.3% Triton-100, blocked with 1% BSA and non-fat milk, and subsequently stained with LC3 (Invitrogen) and DAPI (Vectorshield) and imaged on a Zeiss 710 confocal microscope. All images were collected at the same magnification, scan speed, and line averaging. To segment and count puncta, images were median filtered with a 1x1 kernel, each cell was manually outlined, and the puncta were identified and counted on a per cell basis using the Find Maxima command with 5 set as the noise tolerance. 10 images per condition were imaged to visualize at least 100 cells per condition. For transmission electron microscopy, cells were fixed with 2.5%

glutaraldehyde, 2% paraformaldehyde in 0.1M sodium cacodylate buffer (pH7.2) for 2 hrs and post-fixed with 1% osmium tetroxide for 1.5 hrs at room temperature, then processed in a standard manner and embedded in EMbed 812 (Electron Microscopy Sciences, Hatfield, PA). Semi-thin sections were cut at 1 mm and stained with 1% toluidine blue to evaluate the quality of preservation. Ultrathin sections (60 nm) were cut, mounted on 200 mesh copper grids and stained with uranyl acetate and lead citrate by standard methods. Stained grids were examined under Philips CM-12 electron microscope and photographed with a Gatan (4k x 2.7k) digital camera. Morphometric analysis was performed by analyzing 15-20 different micrographs for each condition. Briefly, multivesicular bodies (MVBs) were identified as round organelles with multiple internal vesicles enclosed within an outer, limiting membrane usually containing an electron-lucent matrix. Lysosomes were identified as spherical organelles frequently containing very tiny granules that are electron dense. Dysmorphic lysosomes (or telolysosomes) were classified as organelles greater than 0.2μm, often asymmetric in shape, containing electron dense material.

SUPPLEMENTAL REFERENCES

Cadwell, K., Patel, K.K., Maloney, N.S., Liu, T.C., Ng, A.C., Storer, C.E., Head, R.D., Xavier, R., Stappenbeck, T.S., and Virgin, H.W. (2010). Virus-plus-susceptibility gene interaction determines Crohn's disease gene Atg16L1 phenotypes in intestine. Cell *141*, 1135-1145.

Glucksberg, H., Storb, R., Fefer, A., Buckner, C.D., Neiman, P.E., Clift, R.A., Lerner, K.G., and Thomas, E.D. (1974). Clinical manifestations of graft-versus-host disease in human recipients of marrow from HL-A-matched sibling donors. Transplantation *18*, 295-304.

Penack, O., Smith, O.M., Cunningham-Bussel, A., Liu, X., Rao, U., Yim, N., Na, I.K., Holland, A.M., Ghosh, A., Lu, S.X.*, et al.* (2009). NOD2 regulates hematopoietic cell function during graft-versus-host disease. J Exp Med *206*, 2101-2110.

Petrovic, A., Alpdogan, O., Willis, L.M., Eng, J.M., Greenberg, A.S., Kappel, B.J., Liu, C., Murphy, G.J., Heller, G., and van den Brink, M.R. (2004). LPAM (alpha 4 beta 7 integrin) is an important homing integrin on alloreactive T cells in the development of intestinal graft-versus-host disease. Blood *103*, 1542-1547.

Figure S1

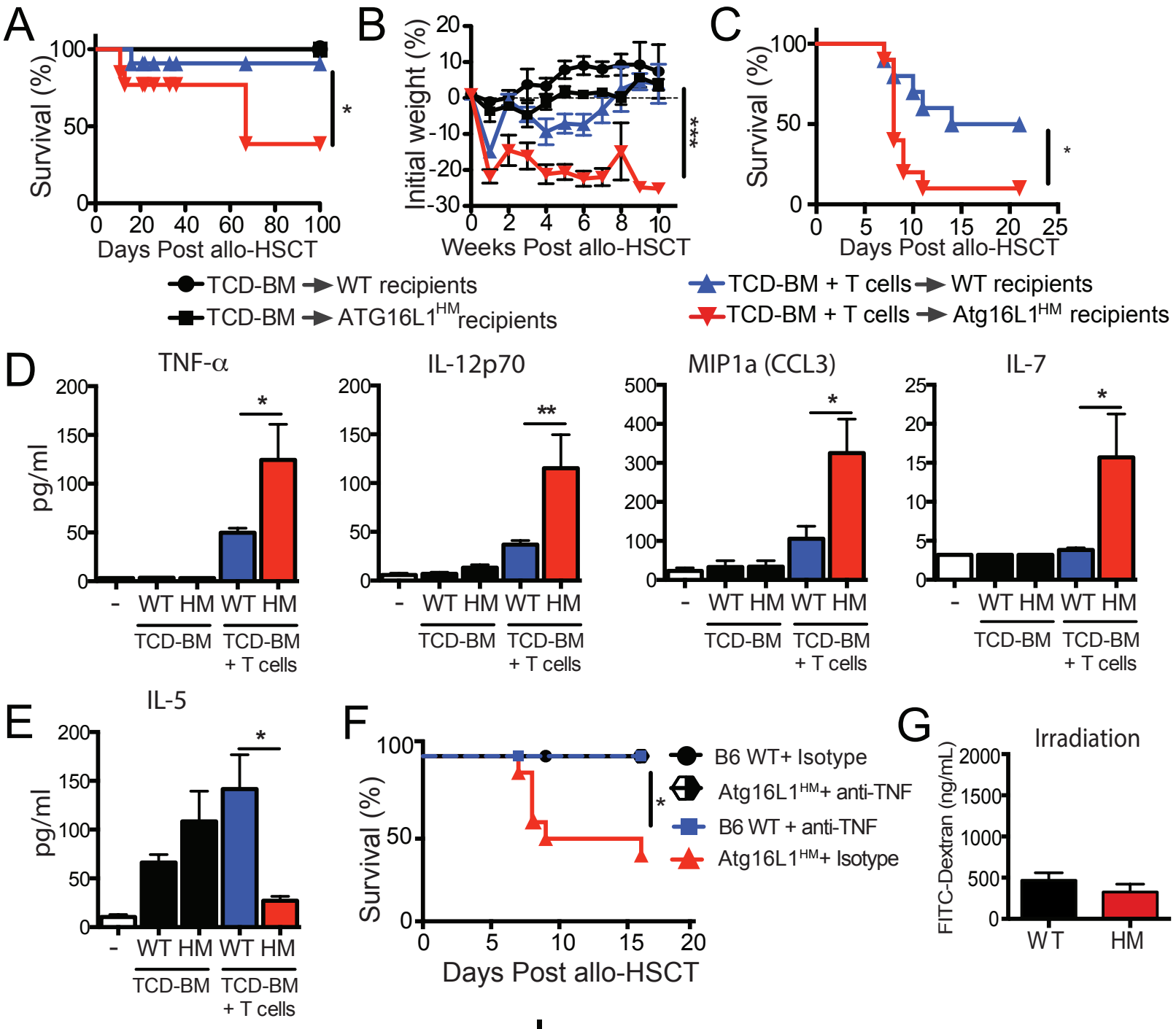
A
Survival (%)
Days Post allo-HSCT
B
Initial weight (%)
Weeks Post allo-HSCT
C
Survival (%)
Days Post allo-HSCT
TCD-BM → WT recipients
TCD-BM → ATG16L1HM recipients
TCD-BM + T cells → WT recipients
TCD-BM + T cells → Atg16L1HM recipients
D
TNF-α
IL-12p70
MIP1a (CCL3)
IL-7
pg/ml
- WT HM WT HM
TCD-BM
TCD-BM + T cells
E
IL-5
F
Survival (%)
Days Post allo-HSCT
B6 WT+ Isotype
Atg16L1HM+ anti-TNF
B6 WT + anti-TNF
Atg16L1HM+ Isotype
G
Irradiation
FITC-Dextran (ng/mL)
WT
HM
H
Cumulative NRM
p = 0.026
Days Post allo-HSCT
Donor ATG16L1 T300A
Donor ATG16L1 wild-type
I
Cumulative NRM
p = 0.1
Days Post allo-HSCT
Recipient ATG16L1 T300A
Recipient ATG16L1 wild-type

Figure S2

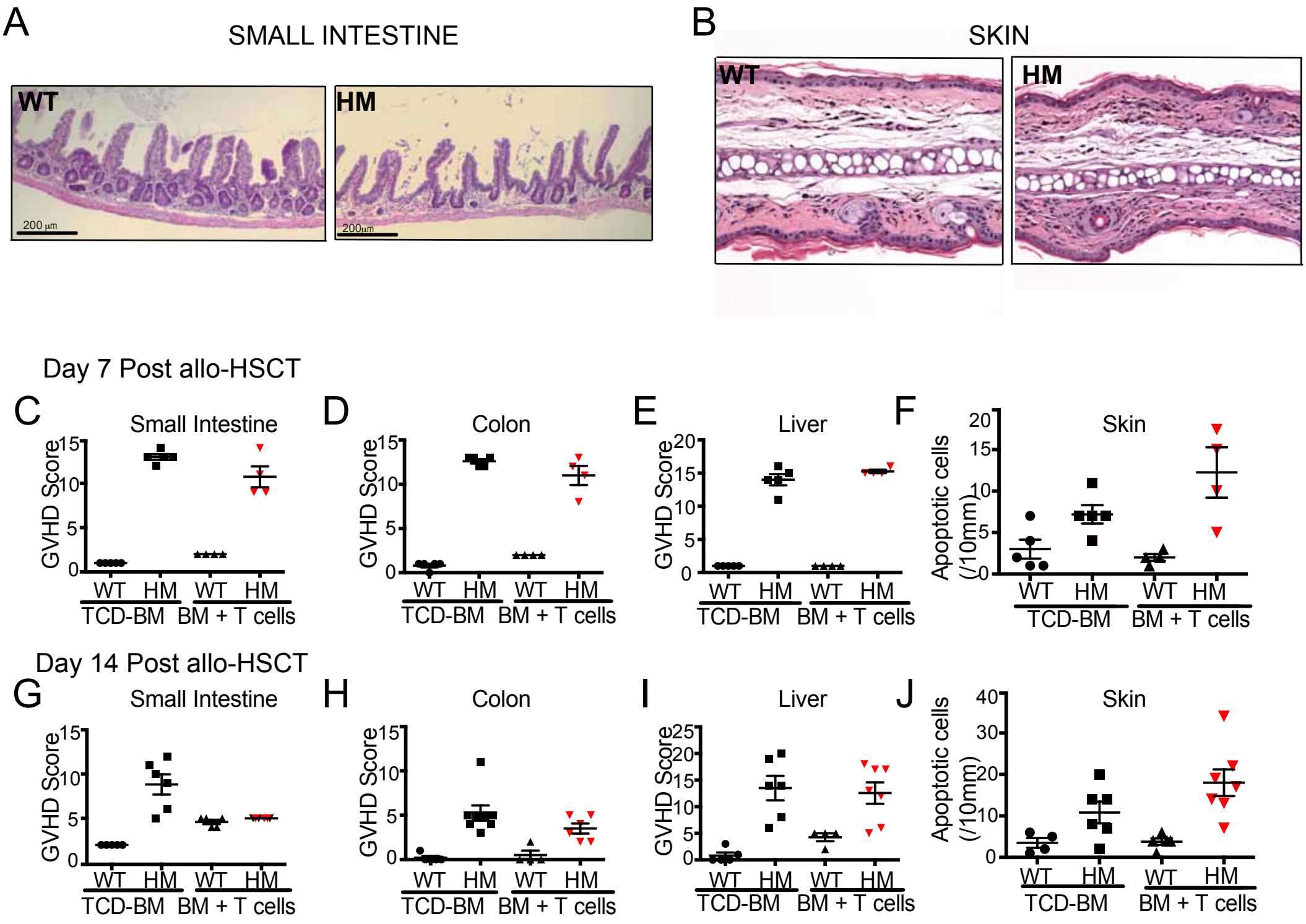
A
SMALL INTESTINE
WT
HM
200 µm
200µm
B
SKIN
WT
HM
Day 7 Post allo-HSCT
C
Small Intestine
GVHD Score
D
Colon
E
Liver
F
Skin
Apoptotic cells (/10mm)
WT HM WT HM
TCD-BM BM + T cells
Day 14 Post allo-HSCT
G
Small Intestine
H
Colon
I
Liver
J
Skin

Figure S3

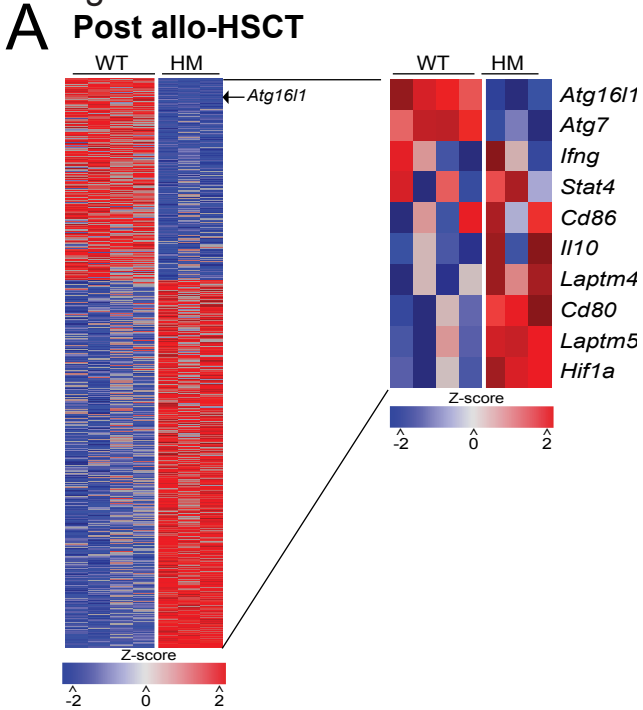

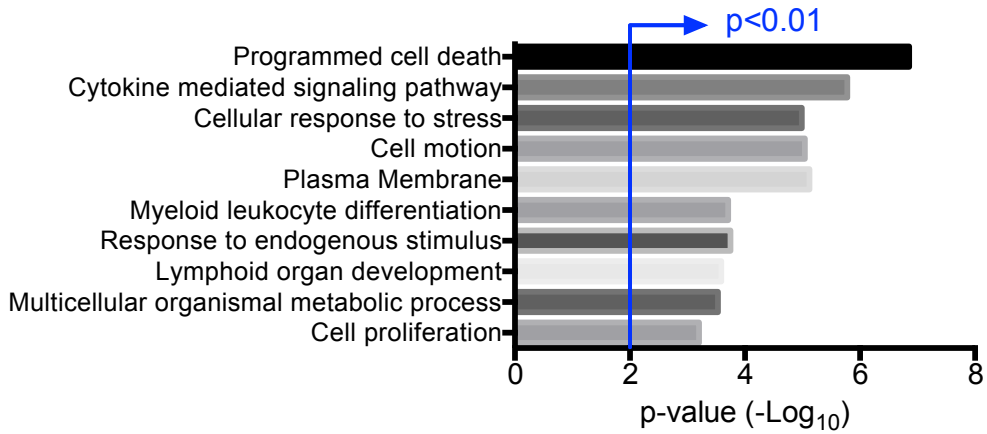

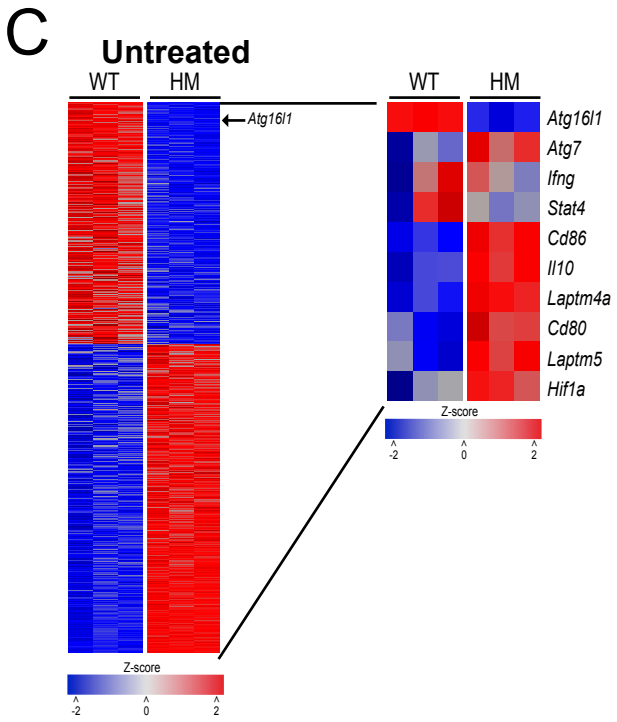

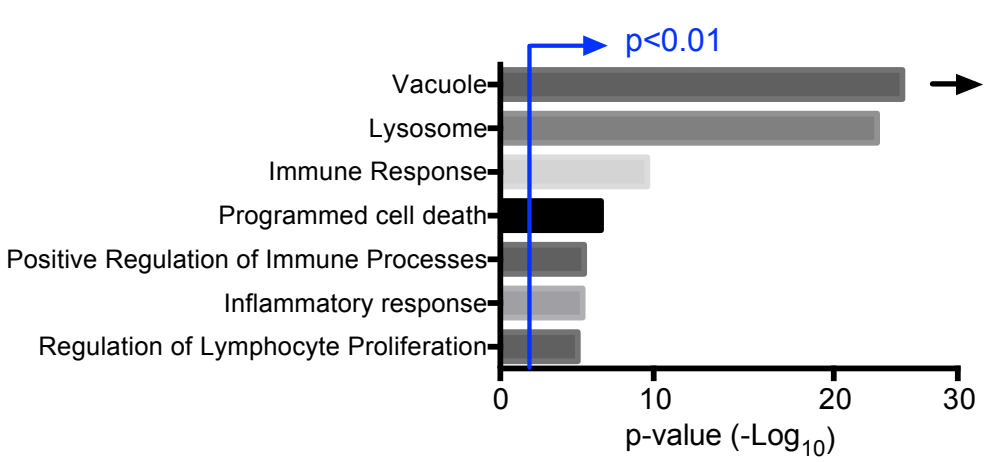

Genes Associated with Autophagy
MAP1LC3A
ATG5
VAMP7
GABARAPL1
GABARAP
LAMP1
LAMP2
DRAM1

FIGURE S4

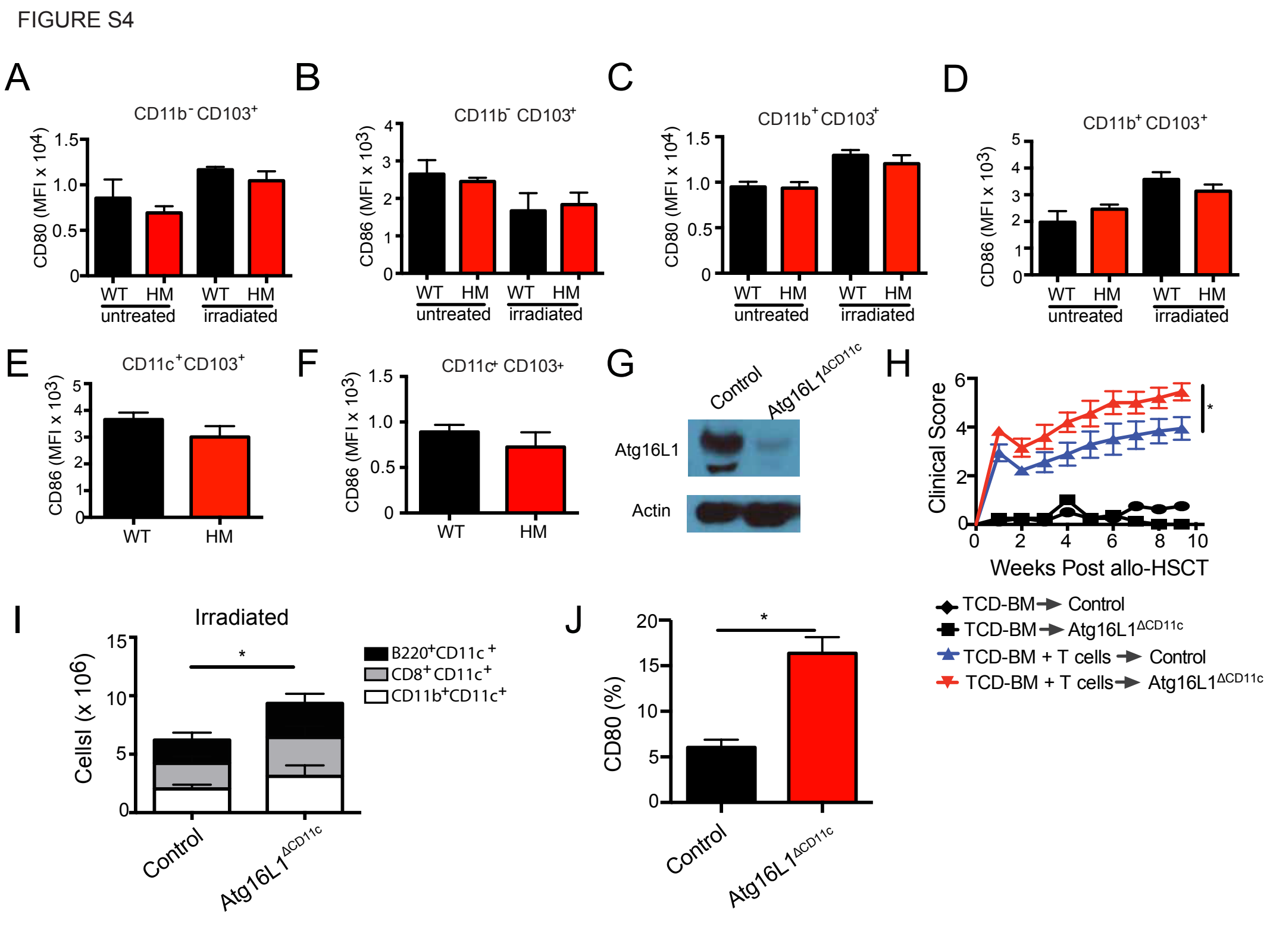
A
CD11b- CD103+
CD80 (MFI x 10^4)
WT HM WT HM
untreated irradiated
B
CD11b- CD103+
CD86 (MFI x 10^3)
WT HM WT HM
untreated irradiated
C
CD11b+ CD103+
CD80 (MFI x 10^4)
WT HM WT HM
untreated irradiated
D
CD11b+ CD103+
CD86 (MFI x 10^3)
WT HM WT HM
untreated irradiated
E
CD11c+ CD103+
CD86 (MFI x 10^3)
WT HM
F
CD11c+ CD103+
CD86 (MFI x 10^3)
WT HM
G
Control
Atg16L1ΔCD11c
Atg16L1
Actin
H
Clinical Score
Weeks Post allo-HSCT
*
TCD-BM → Control
TCD-BM → Atg16L1ΔCD11c
TCD-BM + T cells → Control
TCD-BM + T cells → Atg16L1ΔCD11c
I
Irradiated
Cells (x 10^6)
*
B220+CD11c+
CD8+CD11c+
CD11b+CD11c+
Control
Atg16L1ΔCD11c
J
CD80 (%)
*
Control
Atg16L1ΔCD11c

FIGURE S5

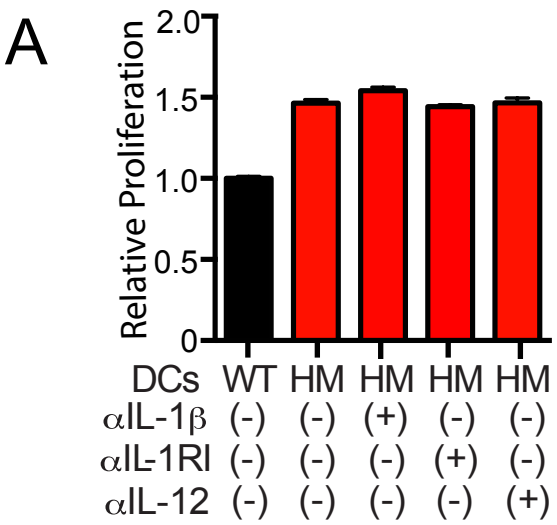
A
Relative Proliferation
2.0
1.5
1.0
0.5
0
DCs WT HM HM HM HM
αIL-1β (-) (-) (+) (-) (-)
αIL-1RI (-) (-) (-) (+) (-)
αIL-12 (-) (-) (-) (-) (+)

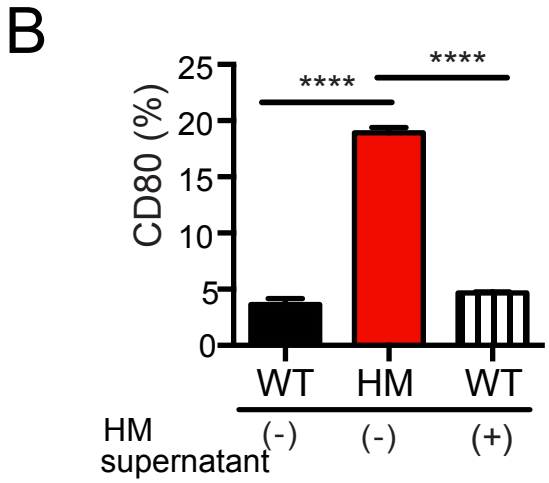
B
CD80 (%)
25
20
15
10
5
0
****
****
WT HM WT
HM supernatant (-) (-) (+)

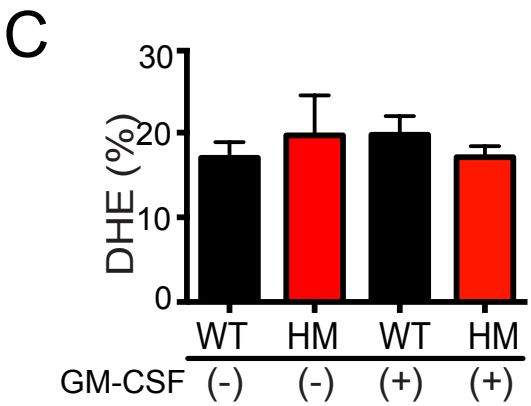
C
DHE (%)
30
20
10
0
WT HM WT HM
GM-CSF (-) (-) (+) (+)

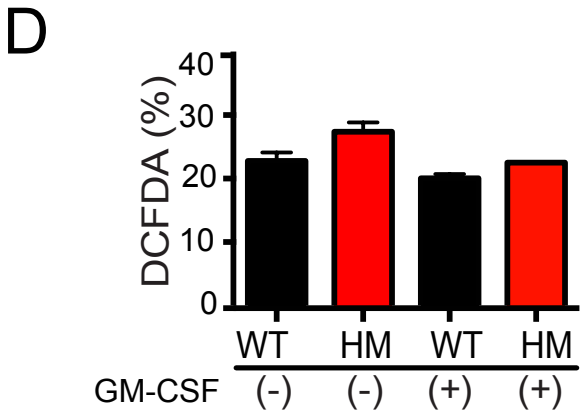
D
DCFDA (%)
40
30
20
10
0
WT HM WT HM
GM-CSF (-) (-) (+) (+)

FIGURE S6

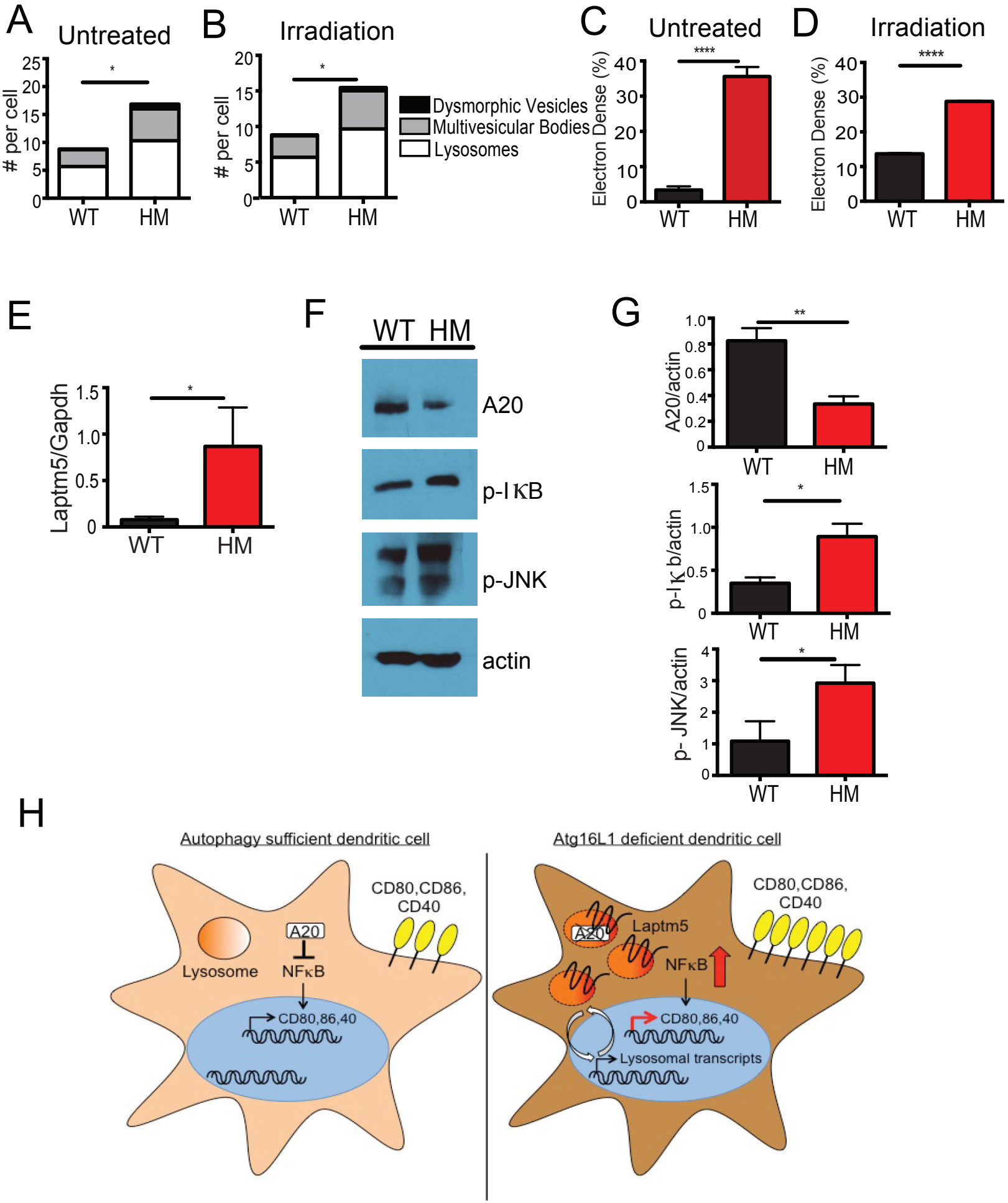
A
Untreated
per cell
WT
HM
B
Irradiation
Dysmorphic Vesicles
Multivesicular Bodies
Lysosomes
C
Untreated
Electron Dense (%)
****
D
Irradiation
E
Laptm5/Gapdh
F
WT HM
A20
p-IκB
p-JNK
actin
G
A20/actin
p-Iκb/actin
p- JNK/actin
H
Autophagy sufficient dendritic cell
Atg16L1 deficient dendritic cell
CD80,CD86,
CD40
Lysosome
A20
NFκB
CD80,86,40
Laptm5
Lysosomal transcripts